Progress In Electromagnetics Research C, Vol. 44, 67–82, 2013

SPECIFIC EMITTER IDENTIFICATION BASED ON TRANSIENT ENERGY TRAJECTORY

Ying-Jun Yuan*, Zhi-Tao Huang, and Zhi-Chao Sha

College of Electronic Science and Engineering, National University of Defense Technology, Changsha, Hunan 410073, P. R. China

Abstract—Specific emitter identification (SEI) is the technique which identifies the individual emitter based on the RF fingerprint of signal. Most existing SEI techniques based on the transient RF fingerprint are sensitive to noise and need different variables for transient detection and RF fingerprint extraction. This paper proposes a novel SEI technique for the common digital modulation signals, which is robust to Gaussian noise and can avoid the problem that different variables are needed for transient detection and RF fingerprint extraction. This makes the technique more practical. The technique works based on the signal's energy trajectory acquired by the fourth order cumulants. A relative smoothness measure detector is used to detect the starting point and endpoint of the transient signal. The polynomial fitting coefficients of the energy trajectory and transient duration form the RF fingerprint. The principal component analysis (PCA) technique is used to reduce the feature vector's dimension, and a support vector machine (SVM) classifier is used for classification. The signals captured from eight mobile phones are used to test the performance of the technique, and the experimental results demonstrate that it has good performance even at low SNR levels.

1. INTRODUCTION

The SEI technique is very significant for the wireless spectrum management, security of Wi-Fi network and cognitive radio network, because the forgery of the RF fingerprint of a specific emitter is difficult as it is comparable to human fingerprint [1]. When an emitter is turned on, the signal goes through a transient state, the transient state

Received 7 August 2013, Accepted 16 September 2013, Scheduled 21 September 2013

* Corresponding author: Ying-Jun Yuan (yuan0410521@gmail.com).

is caused by a combination of effects and has unique and available features for SEI. SEI based on the transient signal requires two key stages: detection of the transients and extraction of the RF fingerprint.

The problem of detection of the transients has been studied as a change point detection problem. In [2], a method based on the variance fractal dimension is reported. This approach is based on the fact that the fractal dimension of the channel noise and the turn-on transient differ from each other. The change in the fractal dimension is then detected by comparing the difference with a threshold. However, the selection of a threshold value is difficult because the noise is variable. In [3], a Bayesian step change detector based on fractal trajectory is reported which does not require a threshold. The method is suited for the VHF radios where there is a step change in the power level at the starting point of transients. However, the output power level of some transients change slowly, e.g., Wi-Fi. For the problem, a Bayesian ramp change detector is reported in [4]. Both approaches in [3, 4] are based on the fact that amplitude features of the channel noise and transient are different, so they are sensitive to noise. Another approach is proposed in [5], based on the fact that the slope of the signal phase becomes and remains linear from the starting point. This method is insensitive to noise and interference, and the detection of starting point of transient signal has an error of about 150 points. In [6, 7], the method of independent component analysis (ICA) is proposed to extract the desired signal from the noise, and it is effective but requires high computation resources.

In some previous researches, the endpoint of transient signal has not been detected. In [8, 9], the end of the transient has been identified in an experimental manner. But in order to estimate the transient duration which can be used as a part of RF fingerprint [10, 11], detection of endpoint is necessary. In [11], the cusum algorithm based on discrete variance has been used to detect the starting point and endpoint. However, an absolute threshold value difficult to confirm is needed.

The RF fingerprint of transient signal has been mainly extracted from the amplitude, frequency, phase and the energy envelope in previous researches. Hall et al. have utilized frequency and amplitude information to create the RF fingerprint for identifying WLAN and Bluetooth transmitters [8, 9]. Afolabi et al. have used a simulation model and formed the RF fingerprints by extracting six features from the preprocessed transient signal using amplitude, phase and frequency profile [12]. VHF radios have been identified by Ellis and Serinken with RF fingerprints created from amplitude and phase information [13]. Xu et al. have used empirical mode decompositions to acquire the

amplitude and time-frequency distribution as RF fingerprint [14]. Ur Rehman et al. have formed the RF fingerprint by extracting six features from the energy envelope [10]. Zhao et al. have used the polynomial fitting coefficients of the energy envelope as the RF fingerprint [15]. Based on wavelet theory, transient signal is decomposed and the coefficients of wavelet have been formed as the RF fingerprint [9, 16].

Mostly, the previous researches are carried out in a laboratory environment. The SNR of signal is usually high, but in a practical application environment, the SNR of the captured signals would be lower, so the susceptibility of the technique to noise should be considered. In many previous researches, the detection of transient and extraction of fingerprint need to calculate different variables, which is not conducive to the practical application.

In this paper, a novel and more practical technique of SEI is proposed. The technique includes a complete classification system: signal acquisition, transient detection, RF fingerprint extraction and classifier. The performance of the technique is tested by the signals from eight mobile phones.

The rest of the paper is organized as follows. In Section 2, the signal acquisition system of mobile phones is illustrated. In Section 3, how the energy trajectory is acquired is explained. In Sections 4 and 5, the extraction process of transient signal and RF fingerprint are explained. Experimental results and conclusion are discussed in Sections 6 and 7, respectively.

2. SIGNAL ACQUISITION

A signal acquisition system, shown in Fig. 1, is designed to collect signals from mobile phones. A digital receiver (20 MHz $\sim$ 4000 MHz) connected to a Yagi antenna converts the radio frequency signals to intermediate frequency (IF) 70 MHz and a Leroy 8500 A digital oscilloscope is used to collect the IF signal. The signals are sampled at a rate of 500 Msps, and the bandwidth of the receiver is 20 MHz. Then the captured signals are transferred to a computer via local area network (LAN) and stored in digital format for further processing. The transient signals are collected from four Nokia 5230, two Motorola Me525 and two Xiaomi mobile phones. The mobile phones work in Global System for Mobile communication (GSM) networks. The radio frequency is 890–909 MHz. The modulation type is minimum shift keying (MSK), and the multiple access is time division multiple address (TDMA). Matlab2009b is used to analyze the transient signals.

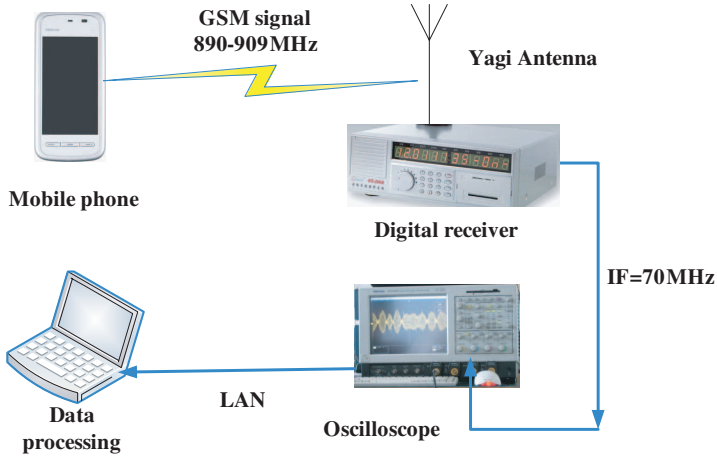

Figure 1. Signal acquisition system.

3. EXTRACTION OF ENERGY TRAJECTORY

3.1. The Basic Knowledge of Higher Order Cumulants

Higher order cumulants (HOC) can describe the higher order statistical characteristic of random process. There is an important feature that the higher order cumulants (greater than second order) of Gaussian noise are permanent zero. So HOC can suppress Gaussian noise. The third order cumulants are permanent zero when the probability density function of signal is symmetrical, so the fourth order cumulants are proposed to detect the transient signal and extract the RF fingerprint in this paper. For a zero-mean complex stochastic process $X(t)$, its p-order hybrid moment can be expressed as follows [17]:

$$M_{pq} = E\left[X\left(t\right)^{p-q} X^{*}\left(t\right)^{q}\right], \tag{1}$$

where * denotes the conjugate function, and the fourth order cumulants of $X(t)$ are calculated as follows [17]:

$$C_{40} = Cum\left(X, X, X, X\right) = M_{40} - 3\left(M_{20}\right)^{2}, \tag{2}$$

$$C_{41} = Cum\left(X, X, X, X^{*}\right) = M_{41} - 3M_{20}M_{21}, \tag{3}$$

$$C_{42} = Cum\left(X, X, X^{*}, X^{*}\right) = M_{42} - \left|M_{20}\right|^{2} - 2\left(M_{21}\right)^{2} \tag{4}$$

Suppose that the signal serial is independent identically distributed, and that E is the signal energy, the fourth order cumulants' theoretical values of the common digital modulation signals are shown in Table 1 [17–19].

Table 1. Theoretical values of the common digital modulation signals' fourth order cumulants.

Modulation type	$\|C_{40}\|$	$\|C_{41}\|$	$\|C_{42}\|$
2ASK	$2E^2$	$2E^2$	$2E^2$
4ASK	$1.36E^2$	$1.36E^2$	$1.36E^2$
BPSK	$2E^2$	$2E^2$	E^2
QPSK	E^2	0	E^2
OQPSK	E^2	0	E^2
$\pi/4-$QPSK	0	0	E^2
(M)PSK$(M>4)$	0	0	E^2
2/4/8FSK	0	0	E^2
MSK	0	0	E^2
GMSK	0	0	E^2
(M)QAM	kE^2 (k depends on M)	0	kE^2 (k depends on M)

3.2. Signal Model

Typical transmission data, such as those shown in Fig. 2, contain Gaussian channel noise followed by the transient signal and the stable signal. So the transmission data can be modeled as follows:

$$d_i = \begin{cases} n(i) & if\ 1 \le i < m \\ s_t(i) + n(i) & if\ m \le i \le k \\ s_s(i) + n(i) & if\ k+1 \le i \le N \end{cases}, \tag{5}$$

where d_i is the data sample at time instant i, N the number of samples, m the starting point of the transient signal, k the endpoint, $n(i)$ the Gaussian channel noise, $s_t(i)$ the transient signal, and $s_s(i)$ the stable signal.

As can be seen from Table 1, the absolute value of C_{42} is kE^2 for the common digital modulation signals, and k depends on the modulation type. So in this paper, the square root of C_{42} is used to acquire the energy trajectory which can express the energy distribution of signal. To acquire the energy trajectory of signal, a sliding rectangular window is used to calculate the local C_{42}. The length of the window is L_{wnd}, and the sliding length is L_{slide}. When

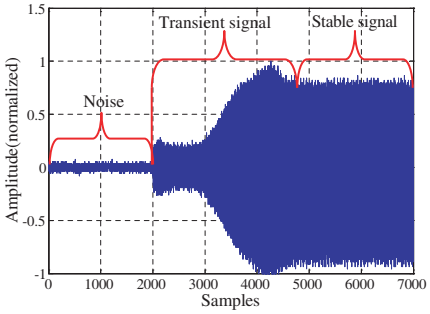

Figure 2. Typical transmission data from a Nokia 5230 mobile phone.

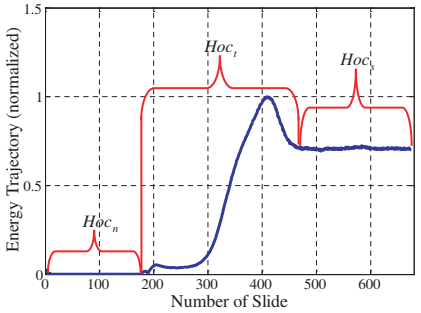

Figure 3. The energy trajectory of the signal shown in Fig. 2.

there are signal and noise in the window, the value of C_{42} only depends on the signal because the nature of HOC expressed as follows:

$$Cum\left[r\left(t\right)\right] = Cum\left[s\left(t\right)\right] + Cum\left[n\left(t\right)\right] = Cum\left[s\left(t\right)\right], \qquad (6)$$

where $r(t) = s(t) + n(t)$, $s(t)$ is signal, $n(t)$ the Gaussian noise, and $s(t)$ and $n(t)$ are independently distributed.

The energy trajectory can be modeled as follows:

$$Hoc\left(i\right) = \begin{cases} Hoc_n\left(i\right) & if\ 1 \le i < m \\ Hoc_t\left(i\right) & if\ m \le i \le k \\ Hoc_s\left(i\right) & if\ k+1 \le i \le N \end{cases}, \qquad (7)$$

where i denotes the i-th slide, $Hoc(i)$ the corresponding $\sqrt{|C_{42}|}$, N the total of slide, m the first time that there is the transient signal in the sliding window, k the last time that there is the transient signal in the sliding window, Hoc_n the $\sqrt{|C_{42}|}$ of noise, Hoc_t the $\sqrt{|C_{42}|}$ of transient signal, and Hoc_s the $\sqrt{|C_{42}|}$ of stable signal. The normalized energy trajectory of the signal shown in Fig. 2 is shown in Fig. 3. The length of the window L_{wnd} is 256, and the sliding length L_{slide} is 10. In order to represent the subtle feature of energy distribution, L_{wnd} and L_{slide} cannot be too large, however L_{wnd} cannot be too small to suppress the Gaussian noise effectively. In this paper, we find that L_{wnd} is $200 \sim 300$ and L_{slide} is $10 \sim 30$ seem to be suitable.

4. TRANSIENT SIGNAL EXTRACTION

Before extracting the transient features, we need to find the exact time when the transient starts and ends. It is significant because inaccurate detection adversely affects the performance of feature extraction.

4.1. Transient Starting Point Detection

As can be seen from formula (7) and Fig. 3, the energy trajectory has obvious characteristics. When there is only noise in the sliding window, theoretically, the value of Hoc_n should be zero, and through experimental verification, it is usually approximate but not zero because the length of the sliding window is not enough. When there is the transient signal in the sliding window, the energy trajectory begins to rise, and when there is only stable signal, the Hoc_s value is stable. Theoretically, $Hoc_s = kE_s$, and E_s is the energy of the stable signal.

In this paper, we use a relative smoothness measure (RSM) detector which has an obvious characteristic at the starting point and endpoint to detect the transients. The other sliding rectangular window is used to calculate the output of the RSM-detector as follows:

$$T(i) = \sum_{j=i}^{i+L_T-1} Hoc(j)^2 \Bigg/ \left(\sum_{j=i}^{i+L_T-1} Hoc(j) \right)^2 \quad 1 \le i \le N - L_T, \quad (8)$$

where i denotes i-th slide, L_T the length of the sliding window, N the length of the energy trajectory, and $T(i)$ the output of the detector. The window slides one point each time. It is obvious that $0 < T(i) \le 1$.

As can be seen from formula (7) and Fig. 3, a hypothesis is reasonable that there is a point $p_s \geqslant m$ (m is the first point of Hoc_t), when $1 \leqslant i \leqslant p_s$, $l > p_s$, $Hoc(l) \gg Hoc(i)$. Because the Hoc_n before m is approximate zero and the energy of transient signal in the i-th ($m \leqslant i \leqslant p_s$) sliding window is little. When $n = p_s + 2 - L_T$, the RSM-detector output value can be approximately calculated as follows:

$$\begin{aligned} T(n) &= \frac{\sum_{j=p_s+2-L_T}^{p_s+1} Hoc(j)^2}{\left(\sum_{j=p_s+2-L_T}^{p_s+1} Hoc(j) \right)^2} \\ &= \frac{\left(\sum_{j=p_s+2-L_T}^{p_s} Hoc(j)^2 + Hoc(p_s+1)^2 \right)}{\left(\sum_{j=p_s+2-L_T}^{p_s} Hoc(j) + Hoc(p_s+1) \right)^2} \approx \frac{Hoc(p_s+1)^2}{Hoc(p_s+1)^2} = 1 \quad (9) \end{aligned}$$

It can be deduced from formula (9) that the RSM-detector will output a maximum near the starting point of the transient signal. Mostly, the transient signal should start before the maximum. In order to find the more exact starting point, a Bayesian change detector in [3]

is used to detect the change point before the maximum. The detector is given as follows:

$$p\left(\{m\}|T\right)\alpha\frac{1}{\sqrt{m\left(N-m\right)}} \times\left[\sum_{i=1}^{N}T(i)^2-\frac{1}{m}\left(\sum_{i}^{m}T\left(i\right)\right)^2-\frac{1}{N-m}\left(\sum_{i=m+1}^{N}T(i)\right)^2\right]^{-\left(\frac{N-2}{2}\right)}, \quad (10)$$

where N is the corresponding point of the maximum, $1 \leqslant m < N$, and $T(i)$ is the i-th RSM-detector output. The energy trajectory of the transient signal shown in Fig. 3 with corresponding RSM-detector output curve ($L_T = 50$) is shown in Fig. 4. The Bayesian method is used to test each point before N as a potential change point using the expression $p(\{m\}|T)$. The corresponding probability density is also shown in Fig. 4.

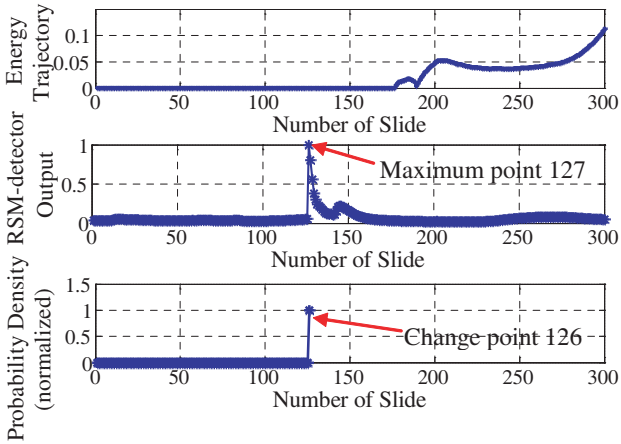

Figure 4. Energy trajectory, RSM-detector curve and change point detection result.

As can be seen from Fig. 4, when the transient signal starts, there is a maximum in the RSM-detector output curve, and the probability density has a peak which is the change point P_c. We can deduce that the transient signal starts at the endpoint of P_c-th sliding window which is used to calculate the RSM-detector output curve. The endpoint of P_c-th sliding window is $P_c + L_T$ in the energy trajectory, which means that the sliding window which is used to get the energy trajectory slides $P_c + L_T$ times. It is reasonable to deduce that the starting point of transient signal is the middle point between

the endpoint of P_c+L_T-1-th and P_c+L_T-th slide. The endpoint of the P_c+L_T-1-th slide in the samples is $(P_c+L_T-2)\times L_{slide}+L_{wnd}$ and the P_c+L_T-th slide is $(P_c+L_T-1)\times L_{slide}+L_{wnd}$. So the starting point in the samples can be calculated as follows:

$$P_{start}=(P_c+L_T-1.5)\times L_{slide}+L_{wnd}, \tag{11}$$

The detected result is 2001 in Fig. 4 and the actual observed value is 2015, so the detection error is 14 samples.

4.2. Transient Endpoint Detection

When the signal is stable, theoretically, $Hoc_s = kE_s$. The RSM-detector output value can be calculated as follows:

$$\begin{aligned} T(n) &= \sum_{j=n}^{n+L_T-1} Hoc(j)^2 \Bigg/ \left(\sum_{j=n}^{n+L_T-1} Hoc(j)\right)^2 \\ &= L_T\times(kE_s)^2 \Big/ (L_T\times kE_s)^2 = 1/L_T, \end{aligned} \tag{12}$$

As can be seen from formula (12), the RSM-detector output value of stable signal only depends on L_T. The stable part of energy trajectory and corresponding RSM-detector curve are shown in Fig. 5. $L_T = 50$, and the theoretical value of $T(n)$ is 0.02.

Through experimental verification, the RSM-detector output values of stable signal are usually approximate but smaller than $1/L_T$.

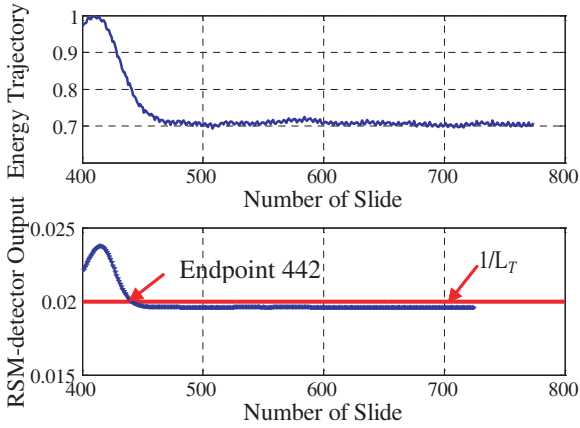

Figure 5. The stable part of energy trajectory and the corresponding RSM-detector output curve.

So the endpoint of transients P_E can be defined as the point that after it nearly all values are smaller than $1/L_T$, which means that all values in the energy trajectory after P_E-th slide are stable. In the P_E-th sliding window, there may be both transient signal and stable signal, so we suppose that the endpoint is the middle point between the starting point and endpoint of P_E-th slide. The starting point of P_E-th slide is $(P_E - 1) \times L_{slide} + 1$, and the endpoint is $(P_E - 1) \times L_{slide} + L_{wnd}$, so the corresponding endpoint in the samples can be calculated as follows:

$$P_{End} = (P_E - 1) \times L_{slide} + 0.5 \times L_{wnd}, \tag{13}$$

The detected result is 4538 in Fig. 4. The actual observed value is 4598, and the detection error is 60 samples.

The duration of transient signal T_d can be calculated as follows:

$$T_d = (P_{End} - P_{start})/Fs, \tag{14}$$

where Fs is the sampling rate and $P_{End} - P_{start}$ the number of samples between the starting point and endpoint of the transient signal.

5. RF FINGERPRINT EXTRACTION AND CLASSIFICATION

5.1. Fingerprint Extraction

As can be seen from Fig. 2 and Fig. 3, the energy trajectory can effectively reflect the characteristics of the transient signal's energy distribution. Eight normalized energy trajectories of the transient signals from different mobile phones are shown in Fig. 6. From the starting point, there are 5,000 samples for each signal and $L_{wnd} = 256$, $L_{slide} = 20$.

As can be seen from Fig. 6, the features of the energy trajectories can be used to form the effective RF fingerprint. The method of least-squares polynomial fitting is used to extract the features from the energy trajectory, and the equation of least-squares polynomial fitting can be expressed as follows:

$$y(x) = a_0 + a_1 x + a_2 x^2 + \ldots + a_n x^n, \tag{15}$$

where $a_0, a_1, a_2, \ldots, a_n$ are the coefficients to be determined, and n is the order of the polynomial function. The fitting function must satisfy the minimum mean-square error (MSE), which can be expressed as follows:

$$MSE = \sum_{i=1}^{N} [y(x_i) - Hoc(i)]^2 \tag{16}$$

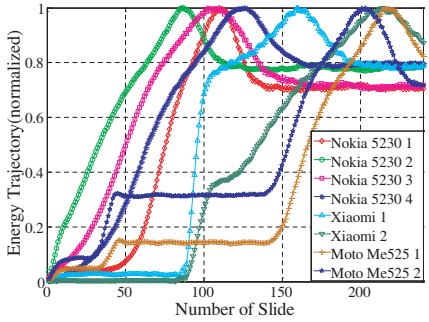

Figure 6. Normalized energy trajectories of transients from eight mobile phones.

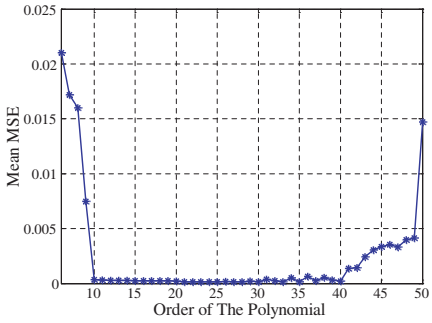

Figure 7. The mean MSE values in different order.

The least-squares algorithm based on QR decomposition (LSQR) presented in [20], which has a more stable behavior and can get a more accurate solution, is used to solve the least-squares problem and get the coefficients.

The order n is important for the performance of the curve fit. In order to find a suitable order n, a set of 160 transient signals are chosen from 8 emitters to test, 20 transient signals from each one. In the experiment, the order n is $6 \sim 50$, and the mean MSE values of curve fit in each n are plotted in Fig. 7.

As can be seen from Fig. 7, when the order is $10 \sim 40$, the MSE is smaller, and that means the performance is better. When the order is higher than 40, the MSE increases because of the waviness and end-effects [21]. The lower the order is, the less the computation is, so the order $n = 10$ in this paper. However, the order depends on the actual situation. When the shape of the energy trajectory is complex or unknown, we suggest the higher order n may be suitable.

When $n = 10$, the 11 polynomial coefficients $a_0, a_1, a_2, \ldots, a_{10}$ are acquired as the feature of energy trajectory. As can be seen from Fig. 6, the duration of transient signal T_d acquired in Section 4 is also an effective feature, so the RF fingerprint feature vector is $[T_d, a_0, a_1, a_2, \ldots, a_{10}]$.

5.2. Reduction of the Feature Vector's Dimension

To reduce the dimension of the feature vector, principal component analysis (PCA) is used in this paper. PCA is a well-known statistical method that has been used in various disciplines for data compression, redundancy and dimension reduction and feature extraction. It can

transform a set of correlated variables into a set of uncorrelated variables, which are ordered by decreasing variability and have a low-dimensional feature vector with low complexity. The low-dimensional feature vector can make the classifier work more effective. The effect of PCA for SEI has been verified [22], and the detailed information about PCA can be found in [22].

5.3. Classification

Support Vector Machine (SVM) is a machine intelligence algorithm based on statistical learning theory, which is popular for pattern recognition. Its core idea is using a pre-selected non-linear mapping to map an linear inseparable space to a linear separable high-dimensional space. In this space, a separating hyperplane with the largest margin can be found using the structural risk minimization principle, and the method of finding the separating hyperplane can maximize the generalization ability of learning machine. The separating hyperplane can maximize the space between different classes [23]. When the data are separable, the classification function is defined as follows:

$$f(x) = sign(w \cdot \phi(x) + b), \tag{17}$$

where $\phi(x)$ is kernel function, and w and b determine the hyperplane of the space. When the data are inseparable, the classification function is defined as:

$$f(x) = sign\left[\left(\sum_{i=1}^{L} \alpha_i y_i K(x_i, x_j)\right) + b\right], \tag{18}$$

where $K(x_i, x_j)$ is kernel function, α_i is i-th mode embedded dimension, y_i is i-th label. Detailed information about SVM can be found in [23–25].

6. EXPERIMENTAL RESULTS

In order to evaluate the performance of this technique, a set of 1200 signals is created by capturing 150 signals from each one of the eight mobile phones. For each emitter, 50 of 150 transients are chosen randomly to create a training set. The remaining 100 transients are used as a test set. Each captured signal includes channel noise, transient and stable signal, and the length is 10000 samples. Firstly, the starting point and endpoint are estimated utilizing the method in Section 4, then the transient energy trajectory is extracted and the feature vector is acquired by polynomial fitting. The method of PCA is used to reduce the dimension of the feature space. A SVM

classifier is created using the feature vectors of the training set, and its performance is evaluated by the feature vectors of the test set.

The signals are captured in a laboratory environment, so the SNRs of the captured signals are high. The detection accuracy of starting point and endpoint is tested using 800 high SNR transient signals. The detection error mean, which is the mean of the difference between the visually observed value and the estimated value, is 16 samples for the starting point and 50 samples for the endpoint. When the high SNR training and test signals arere applied to the classifier, the identification rate is 99.5%.

In a practical application environment, the SNRs of the captured signals will be lower. To test the performance at lower SNR levels, the signals with SNR values of 10–20 dB are synthesized using the "awgn" function of Matlab2009b, which can add Gaussian white noise to signals. The detection errors in different SNRs are shown in Fig. 8.

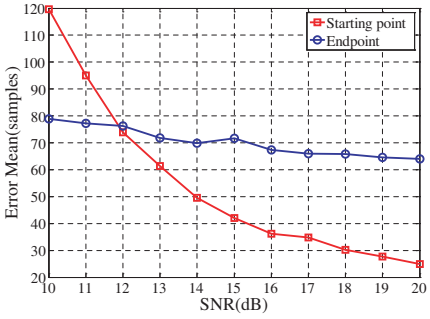

Figure 8. Detection error means of the starting point and endpoint.

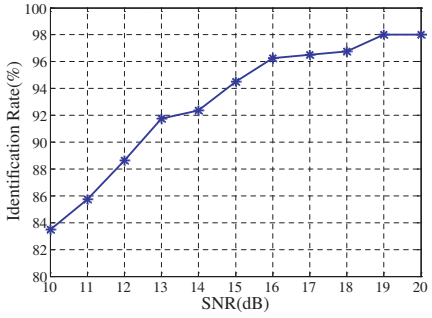

Figure 9. Identification rate of different SNR.

In [26], Tekbas et al. have discussed the method that can improve the identification performance at low SNR levels. Firstly, a limited number of classifiers are trained by the training sets with different SNRs. Then each noisy test transient is classified using the classifier having the nearest SNR value. The performance improvement is verified with experimental data. So in this paper, we use this method to test the performance at lower SNR levels. For the test signals with SNR values of 10–20 dB, three SVM classifiers are trained by three sets of 10, 15, 20 dB, respectively. The test signals are classified by the classifier with nearest SNR value. The classification result for different SNR is shown in Fig. 9.

As can be seen from Fig. 8, the detection error means of the starting point and endpoint are less than 100 samples at 500 Msps when

SNR > 10 dB. But the detection error mean increases fast when SNR reduces for the starting point detection and slowly for the endpoint detection because the energy at the starting point is so small that it can be affected by noise more easily. As can be seen from Fig. 9, the identification rate is more than 90% when SNR > 12 dB.

7. CONCLUSION

In this paper, a more practical SEI technique for the common digital modulation signals shown in Table 1 is proposed. The technique detects the transients and extracts the RF fingerprint based on the energy trajectory of signal, and then a SVM classifier is used to identify eight mobile phones.

In this technique, a RSM-detector is used to detect both starting point and endpoint of transient signal, which does not need an absolute threshold and has good performance. The energy trajectory of signal is used to detect the transients and extract the RF fingerprint. The problem that different variables are needed for transient detection and RF fingerprint extraction is avoided. The energy trajectory is acquired by fourth order cumulants which can suppress Gaussian noise, so the technique is robust to Gaussian noise. In order to test the performance at low SNR levels, the signals with SNR values of 10–20 dB are used to test. The experimental results demonstrate that the technique has good performance at low SNR.

REFERENCES

1. Danev, B., H. Luecken, S. Capkun, and K. EI Defrawy, "Attacks on physical-layer identification," *Proc. ACM Conf. on Wireless Network Security*, 89–98, 2010.
2. Shaw, D. and W. Kinsner, "Multifractal modeling of radio transmitter transients for classification," *Proc. WESCANEX'97*, 306–312, 1997.
3. Ureten, O. and N. Serinken, "Detection of radio transmitter turn-on transients," *Electronics Letters*, Vol. 35, No. 23, 1996–1997, 1999.
4. Ureten, O. and N. Serinken, "Bayesian detection of Wi-Fi transmitter RF fingerprints," *Electronics Letters*, Vol. 41, No. 6, 373–374, 2005.
5. Hall, J., M. Barbeau, and E. Kranakis, "Detection of transient in radio frequency fingerprinting using signal phase," *Proceedings*

of the 3rd IASTED Int. Conf. on Wireless and Optical Communications, 13–18, 2003.

6. Lee, T. W., *Independent Component Analysis: Theory and Applications,* Kluwer Academic Publishers, 1999.
7. Donelli, M., "A rescue radar system for the detection of victims trapped under rubble based on the independent component analysis algorithm," *Progress In Electromagnetics Research M*, Vol. 19, 173–181, 2011.
8. Hall, J., M. Barbeau, and E. Kranakis, "Enhancing intrusion detection in wireless networks using radio frequency fingerprinting," *Proceedings of the 3rd IASTED International Conference on Communications, Internet and Information Technology (CIIT)*, 201–206, 2004.
9. Hall, J., M. Barbeau, and E. Kranakis, "Detecting rogue devices in bluetooth networks using radio frequency fingerprinting," *IASTED International Conference on Communications and Computer Networks*, 108–113, 2006.
10. Ur Rehman, S., K. Sowerby, and C. Coghill, "RF fingerprint extraction from the energy envelope of an instantaneous transient signal," *Australian Communications Theory Workshop (AusCTW)*, 90–95, 2012.
11. Bonne Rasmussen, K. and S. Capkun, "Implications of radio fingerprinting on the security of sensor networks," *Proceedings of the Third International Conference on Security and Privacy in Communications Networks and the Workshops, IEEE*, 331–340, 2007.
12. Afolabi, O., K. Kim, and A. Ahmad, "On secure spectrum sensing in cognitive radio networks using emitters electromagnetic signature," *Proceedings of 18th Internatonal Conference on Computer Communications and Networks*, 1–5, 2009.
13. Ellis, K. and N. Serinken, "Characteristics of radio transmitter fingerprints," *Radio Science*, Vol. 36, No. 4, 585–597, 2001.
14. Xu, J., H. Zhao and T. Liang, "Method of empirical mode decompositions in radio frequency fingerprint," *2010 International Conference on Microwave and Millimeter Wave Technology (ICMMT)*, 1275–1278, 2010.
15. Zhao, C., L. Huang, L. Hu, and Y. Yao, "Transient fingerprint feature extraction for WLAN cards based on polynomial fitting," *The 6th International Conference on Computer Science & Education (ICCSE 2011)*, 1099–1102, 2011.
16. Klein, R. W., M. A. Temple, and M. J. Mendenhall, "Application

of wavelet-based RF fingerprinting to enhance wireless network security," *Journal of Communications and Networks*, 544–555, 2009.

17. Wang, L. and Y. Ren, "Recognition of digital modulation signals based on high order cumulants and support vector machines," *ISECS International Colloquium on Computing, Communication, Control, and Management*, 271–274, 2009.
18. Zhou, X., Y. Wu, and B. Yang, "Signal classification method based on support vector machine and high-order cumulants," *Wireless Sensor Network*, 48–52, 2010.
19. Swami, A. and B. M. Sadler, "Hierarchical digital modulation classification using cumulants," *IEEE Transactions on Communications*, Vol. 48, No. 3, 416–429, 2000.
20. Paige, C. and M. Saunders, "LSQR: An algorithm for sparse linear equations and sparse least squares," *ACM Trans. Math. Software*, Vol. 8, 43, 1982.
21. Robert-Granie, C., J.-L. Foulley, E. Maza, and R. Rupp, "Statistical analysis of somatic cell scores via mixed model methodology for longitudinal data," *Anim. Res*, Vol. 53, 259–273, 2004.
22. Xu, S., B. Huang, L. Xu, and Z. Xu, "Radio transmitter classification using a new method of stray features analysis combined with PCA," *Military Communications Conference (MILCOM 2007)*, 1–5, 2007.
23. Burges, C. J. C., "A tutorial on support vector machines for pattern recognition," *Data Mining and Knowledge Discovery*, 121–167, 1998.
24. Bermani, E., A. Boni, A. Kerhet, and A. Massa, "Kernels evaluation of SVM-based estimators for inverse scattering problems," *Progress In Electromagnetics Research*, Vol. 53, 167–188, 2005.
25. Bermani, E., A. Boni, S. Caorsi, M. Donelli, and A. Massa, "A multi-source strategy based on a learning-by-examples technique for buried object detection," *Progress In Electromagnetics Research*, Vol. 48, 185–200, 2004.
26. Tekbas, O. H., O. Ureten, and N. Serinken, "Improvement of transmitter identification system for low SNR transients," *Electronics Letters*, Vol. 40, No. 3, 192–183, 2004.